AD-A149 236 THE USE OF ADHESIVE-BONDED RIVETS TO LESSEN THE REDUCTIONS IN FATIGUE LIF..(U) AERONAUTICAL RESEARCH LABS MELBOURNE (AUSTRALIA) J Y MANN ET AL. MAR 84 1/1

UNCLASSIFIED ARL-STRUC-399 F/G 13/5 NL

END
DATE
FILMED
2 85
DTIC

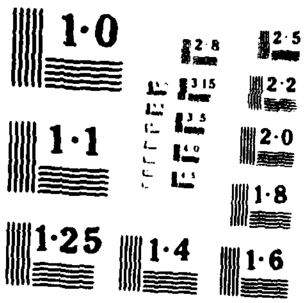
1·0
2·8
2·5
2·2
1·1
2·0
1·8
1·25
1·4
1·6

ARL-STRUC-REPORT-399 AR-003-011

AD-A149 236

DEPARTMENT OF DEFENCE

DEFENCE SCIENCE AND TECHNOLOGY ORGANISATION

AERONAUTICAL RESEARCH LABORATORIES

MELBOURNE, VICTORIA

STRUCTURES REPORT 399

THE USE OF ADHESIVE-BONDED RIVETS TO LESSEN THE REDUCTIONS IN FATIGUE LIFE CAUSED BY RIVET HOLES

by

J. Y. MANN, R. A. PELL, R. JONES and M. HELLER

APPROVED FOR PUBLIC RELEASE

COPY No 84 12 31 041 MARCH 1984

AR-003-011

DEPARTMENT OF DEFENCE
DEFENCE SCIENCE AND TECHNOLOGY ORGANISATION
AERONAUTICAL RESEARCH LABORATORIES

STRUCTURES REPORT 399

THE USE OF ADHESIVE-BONDED RIVETS TO LESSEN THE REDUCTIONS IN FATIGUE LIFE CAUSED BY RIVET HOLES

by

J. Y. MANN, R. A. PELL, R. JONES and M. HELLER

SUMMARY

Rivet holes are potential sites for fatigue crack initiation in aircraft structures. Several methods for improving the life of such details were investigated including coating the surface of the hole with adhesive, cold-expansion of the holes, the insertion of close-fit rivets and the use of adhesively-bonded rivets.

Of the various techniques examined only that involving adhesively-bonded rivets provided any significant improvements in fatigue life. It resulted in a reduction in fatigue crack propagation rate of about 50% compared with that for specimens incorporating open holes.

A finite element analysis indicated that adhesive bonding significantly reduces both the local stress concentration at the hole and the stress intensities at the crack tips, thus retarding crack initiation and reducing fatigue crack propagation rates. However, the effective reduction in stress intensity resulting from bonding (about 17%) is much less than the 50% predicted by the finite element analysis. This discrepancy is attributed mainly to shortcomings in the model for defining the characteristics and behaviour of the adhesive.

POSTAL ADDRESS: Director, Aeronautical Research Laboratories,
Box 4331, P.O., Melbourne, Victoria, 3001, Australia

CONTENTS

A-1

1. INTRODUCTION

During the full-scale fatigue testing of Mirage III fighter wings at the Swiss Federal Aircraft Factory (F + W), Switzerland, fatigue cracks were discovered at the innermost bolt holes along the rear flanges of the main spars. Subsequently, crack indications were confirmed at identical locations in wings of the Royal Australian Air Force Mirage IIIO fleet (Ref. 1). As a consequence, several investigations were undertaken at the Aeronautical Research Laboratories (ARL) to explore methods for increasing the fatigue lives at critical sections of the spars (Refs 1-3).

An area in the wing main spar of particular concern was the first bolt hole in the lower rear flange. A detail of the spar in this region is shown in Fig. 1. The development of a life-enhancement scheme for this portion of the spar was complicated by the presence of two through-the-flange single-leg-anchor-nut (SLAN) rivet holes located close to the bolt hole in a chordwise direction. Although the installation of interference-fit steel bushes at the bolt hole virtually inhibited crack initiation at the bolt hole (Refs 1, 2) and the adoption of a modified system for securing the SLAN obviated the need for through-the-flange rivets, a consequence was that the SLAN rivet holes then became the critical locations for fatigue crack initiation. Several alternatives including reaming, cold-expanding and the insertion of close-fit rivets were tested as part of the main life-enhancement investigation for the spar, but these did not provide any significant improvements in life for cracks which initiated at the rivet holes.

Adhesive bonding of close-fit rivets in the SLAN holes was then proposed as a method of improving fatigue life. This was based on the premise that the adhesive would result in better load transfer through the rivet (and in so doing reduce the stress concentrating effect of the hole) and, subsequent to crack initiation, reduce the stress intensity at the crack tip (Ref. 4). In addition, the adhesive could act as an environmental barrier (Ref. 5), or provide an interlayer which would reduce the effects of fretting between the rivet and hole surface. The proposal was investigated in two complementary series of fatigue tests which are covered by this report.

2. SPECIMENS AND TESTING PROGRAM

Figure 2 illustrates the basic forms of the two types of fatigue specimens employed in this investigation. The use of two types was necessitated by the availability at the time of suitable test material. Type (a) being made from offcuts of B.S. L168* aluminium alloy extruded bar 63.5 mm × 31.75 mm in section (Serial GR) used for the investigation reported in Reference 6, while Type (b) were taken from offcuts of 32 mm thick 2014-T651* aluminium alloy rolled plate (Serial GJ) covered by Reference 3. In both cases the axis of the specimen was parallel to the direction of extrusion/rolling of the material. The chemical compositions, tensile properties and fracture toughness of the materials are given in Appendix I.

2.1 Type (a) specimens (total 21)

In these specimens, the pitch between the twin holes was the same as the nominal pitch of the two rivet holes in the SLAN, and the distance from the centre line of each hole to the closest side of the specimen was that from the inner side of the 8 mm spar bolt hole to the centre line of the first rivet hole i.e. 8.70 mm. A specimen thickness of 30 mm was chosen to correspond to the thickness of the spar flange at the SLAN section.

* The chemical compositions and static properties of these materials are equivalent to those of the French alloy A-U4SG used for the manufacture of the spars.

Eight different hole treatments were investigated.

(i) Holes drilled 3·3 mm diameter, 0·125 inch diameter universal head rivets inserted against a packing piece, with the tail of the rivet peened into the countersink. This generally represented the original condition in the RAAF Mirage IIIO wings.

(ii) Holes drilled 3·3 mm diameter and left empty. A condition equivalent to that of rivet removal from the spar flange without any reworking of the rivet holes.

(iii) Holes reamed to 4 mm diameter and left empty. Representing a situation in which the rivet holes were simply cleaned up for inspection.

(iv) Holes as in (iii) incorporating selected 5/32 inch (4 mm) diameter countersink-head 2117 aluminium alloy rivets pressed-in by hand to provide a neat fit. Designed to allow some load transfer through the rivet but to enable easy rivet removal for hole inspection during testing if required.

(v) Holes and rivets as in (iv), but with rivets permanently bonded in position using an epoxy adhesive Type K 138.*

(vi) Holes cold-expanded using the Boeing split-sleeve process (Ref. 7) to finish at 4 mm diameter.* Holes left empty. The cold-expanding process introduces a residual compressive stress field adjacent to the hole which can retard fatigue crack initiation and growth.

(vii) Holes as in (vi) but incorporating close-fit rivets as in (iv).

(viii) Holes and rivets as in (vii) but with rivets adhesively bonded as in (v).

2.2 Type (b) specimens (total 9)

In these specimens the distance from the centre line of the hole to the side of the specimen (8·70 mm) corresponded to that in the Type (a) specimens. The specimen thickness was, however, slightly less i.e. 28 mm. Four hole treatments were investigated.

(i) Holes reamed to 4 mm diameter and left empty. Equivalent to Type (aiii).

(ii) Holes reamed as in (i) and left empty, but a coating of adhesive applied to the hole surface.

(iii) Holes reamed as in (i) but incorporating pressed-in close-fit rivets. Equivalent to Type (aiv).

(iv) Holes reamed as in (i) but incorporating adhesive-bonded close-fit rivets. Equivalent to Type (av).

3. FATIGUE TESTS

The multi-load-level fatigue testing sequence adopted for this investigation was identical to that used for the other Mirage life-enhancement programs (Refs 1-3, 6). It consisted of a 100-flight sequence of four different flight types as indicated in Fig. 3. Cycles of +6·5 g/ −1·5 g and +7·5 g/ −2·5 g (a total of 39 cycles in 100 flights) were applied at a cyclic frequency of 1 Hz, whereas the remaining 1950 cycles per 100 flights were at 3 Hz. Sine-wave loading was adopted throughout. All fatigue tests were carried out in a Tinius-Olsen servo-controlled electro-hydraulic fatigue machine, the 100-flight sequence being achieved using an EMR Model 1641 programmable function generator controlled by a punched tape.

---

* Details of the hole preparation, etc. for the adhesive-bonding and cold-expansion processes are given in Appendix 2.

For Type (a) specimens fatigue loads were based on the assumption that $+7 \cdot 5$ g corresponded to a gross-area stress of 235 MPa (34 100 psi) and that there was a linear stress/g relationship i.e. the 1 g gross-area stress was 31·3 MPa (4547 psi). This magnitude of stress was chosen on the basis of results from a previous investigation (Ref. 6) using the same batch of material so that individual fatigue specimens should have test durations of between about one and two days. Specimens with 3·3 mm diameter holes had a nominal nett area of 562 mm^2, while those with 4 mm holes a nett area of 520 mm^2. The resulting nett area stresses were 318 MPa (46 100 psi) and 344 MPa (49 900 psi) respectively – a difference of about 8%.

The nett area stress chosen for the Type (b) specimens was the same as that for Type (a) specimens incorporating 4 mm holes, i.e. 344 MPa (49 900 psi). In this case the gross area stress was 265 MPa (38 390 psi).

Tables 1 and 2 give the individual fatigue lives, log. average lives and standard deviations of log. life for the various groups of Type (a) and Type (b) specimens. The extent of the fatigue cracking and representative fractures for Type (a) specimens are illustrated in Figs 4 and 5 respectively, while similar information relating to Type (b) specimens is shown in Figs 6 and 7.

4. DISCUSSION

The individual fatigue test series involving the twin hole and single hole specimens both demonstrate the effectiveness of adhesive-bonded rivets in providing a significant increase in the life to failure relative to those for other hole treatments. Compared with specimens having reamed open holes, the ratio of lives for specimens incorporating adhesive-bonded rivets in reamed holes are 2·65 and 2·61 for the twin-hole and single-hole specimens respectively. On the limited data available, the cold-expansion of the holes in the twin-hole specimens does not result in a significant increase in life compared with that of reamed open-hole specimens, but bonding of rivets in cold-expanded holes again provides a marked increase in life. Furthermore, an adhesive coating on the hole surface of the single-hole specimens has not resulted in an improvement in life.

For both types of specimens the lives of those incorporating pressed-in rivets were not significantly different to those of open-hole specimens with similar hole conditions. On the basis of nett area stresses, the 4 mm reamed open twin-hole specimens would have been expected (Ref. 6) to have an average life of about 55% that of the 3·3 mm drilled hole specimens, i.e. 4200 flights. The greater actual life (5929 flights) of the reamed hole specimens probably reflects the much better hole surface finish in these compared with the drilled-hole specimens.

Three reasons which could be advanced for the significant improvement in life associated with the use of adhesive-bonded rivets are:

(a) the adhesive acting as a barrier to inhibit crack initiation which might otherwise have been accelerated by environmental interaction;

(b) the adhesive acting as a non-metallic interlayer, thus separating the rivets and hole surface and reducing the potentially deleterious effects of fretting;

(c) the adhesive providing improved load transfer characteristics at the section, both before and after crack initiation.

The tests on single-hole specimens suggest that the adhesive coating, as such, does not play a major part in the increased life associated with adhesive-bonded rivets. An examination of the fracture surfaces of specimens with filled holes (i.e. incorporating either pressed-in or adhesive-bonded rivets) indicated the presence of fretting at or close to the countersink-end of nearly every hole, with lesser or no fretting at the other end of the holes. Of the 20 'filled-hole' specimens (15 twin-hole and five single-hole) the primary crack initiation in 13 was some distance from the ends of the hole and in the other four close to the end opposite to the countersink.

It was only in the other three cases (one twin-hole cold-expanded, adhesive-bonded specimen No. GR22B, and two single-hole one each with pressed-in and adhesive-bonded rivets, GJ1Z and GJ1ZA respectively) that the primary crack developed from close to the countersink and fretting apparently did play a significant part in its initiation. Thus, as fretting was not a major factor in crack initiation in the non-adhesive-bonded specimens, the anti-fretting properties of the adhesive interlayer are unlikely to be responsible for the benefits resulting from the use of adhesive-bonded rivets.

An improved load transfer at the section containing the holes would be expected to delay the initiation of fatigue cracks by reducing the effective stress concentration and, providing the continuity of the adhesive was maintained, to reduce the fatigue crack propagation rate because of a reduction in the stress intensity at the crack tip. In order to elucidate this matter fractographic crack growth studies were made on several single-hole specimens (these being chosen in preference to the twin-hole specimens because of their less complicated crack development and to avoid problems associated with crack interactions which were apparent when two holes were present), and a complementary finite-element analysis made of the stress distributions around uncracked and cracked open holes and holes containing adhesively-bonded rivets.

One specimen from each of the four single-hole types was selected for detailed fractographic examination, and the respective fracture surfaces are illustrated in Fig. 7. It is clear that there are significant differences in crack development in these four specimens, and although a basis for selection was that of approximately equal maximum crack depths on both sides of the hole this criterion could not be satisfied in the case of the specimen with a pressed-in rivet (Type (biii)). The fracture surface feature used as the reference for crack growth measurements was that produced by the 7·5 g load which occurs only once in the 100-flight sequence, during flight 42. In every case growth data were obtained for the cracks initiating at both sides of the hole.

Details of the fractographic techniques employed are given in Appendix 3. These included the use of macrophotographs, an optical stereo microscope and a metallographic microscope. Crack growth measurements were obtained at distances as close as 0·020 to 0·039 mm from the hole surface in the case of specimens with open holes and pressed-in rivets and 0·125 mm in the case of the specimens with adhesive-bonded rivets. The incremental crack growth data obtained using the three techniques were combined to provide the series of crack growth plots illustrated in Fig. 8, and the curves (for the longer crack in each of the four specimens) shown in Fig. 9.

These curves show that the fatigue crack propagation period covers a much greater part of the life in adhesively-bonded rivet specimens than in the other three types of specimens. However, as the maximum crack depth for a given crack geometry is defined by the fracture toughness of the material, no great differences in the crack growth characteristics between the four types of specimens would have been anticipated at crack depths approaching complete fracture. Because of the absence of definable features on the fracture surfaces of adhesive-bonded specimens at crack depths of less than 0·125 mm, the fractographic studies did not provide any evidence relating to the effects of adhesive bonding on fatigue crack initiation in these specimens.

The fractographic crack growth measurements also allowed the determination of the incremental crack propagation rates at the different crack depths corresponding to the applications of the 7·5 g load. Two specimens were selected for detailed analysis. They were the open-hole specimen No. GJ1ZB and the adhesively-bonded rivet specimen No. GJ2B16, each of which had reasonably symmetric crack growth from both sides of the hole. This allowed the crack growth data for both sides of the holes in the individual specimens to be pooled. The crack depth versus incremental crack growth data were plotted on linear scales and second order polynomial curves fitted. (It should be noted however that there was considerable variability in the raw incremental growth data for crack depths of greater than about 2 mm). Calculated crack growth rates at selected crack depths are given in Table 3.

On the premise that (for similar crack geometries) any given crack propagation rate represents conditions of equivalent stress intensity factors in the two types of specimens, it can be seen from Table 3 that 0·5, 1·0, 1·5 and 2·0 mm deep cracks in adhesively-bonded rivet specimens are equivalent to those of 0·2, 0·6, 1·0 and 1·4 mm in depth respectively in open-hole specimens. Clearly, the percentage reduction in crack propagation rate associated with the use of bonded rivets decreases as the cracks become deeper, and would approach zero at final fracture

conditions. Using data for a similar material published elsewhere. (Ref. 9) it was estimated that a reduction in fatigue crack propagation rate of 50% should represent a reduction in stress intensity at the crack tip of about 17%. Reductions of about 50% in crack propagation rate are evident for the open-hole specimen when comparing the rates at crack depths of 2·0 and 1·1 mm, and 1·0 and 0·5 mm; and for the adhesive-bonded rivet specimen at depths of 2·2 and 1·3 mm, and 1·2 and 0·7 mm. At a crack depth of 0·5 mm the crack growth rate in the bonded-rivet specimen is about half that in the open hole specimen.

In order to understand the mechanisms which resulted in the increase in fatigue life of the adhesively-bonded specimen a detailed finite element analysis (Ref. 10) was undertaken on the single-hole specimen containing a bonded rivet. Initially the specimen was considered to be uncracked and, due to symmetry, only a quarter of it was modelled. The resultant plane strain finite element model consisted of 38 eight-noded isoparametric quadrilateral elements and eight six-noded isoparametric triangular elements (see Fig. 10(*a*)). Element stiffness matrices were computed using reduced integration and double precision and the solution was also performed using double precision.

The aluminium alloy rivet and specimen were both assumed to have a Modulus of Elasticity of 73 000 MPa and a Poisson's ratio of 0·32, while the adhesive was assumed to have a Modulus of Elasticity of 700 MPa and a Poisson's ratio of 0·35. The adhesive layer was very thin and although its thickness was not precisely known it was, for the purpose of this analysis, taken to be 0·0127 mm. It was assumed that the applied tensile stress corresponded to the maximum load of 7·5 g in the fatigue sequence. This resulted in a gross area 'applied' stress of 265 MPa and a nett section stress at the hole of 344 MPa.

Unfortunately no information on the static tensile or fatigue strength of the adhesive was available and so two separate analyses were undertaken where:

(i) the adhesive was assumed to not yield or fail,

(ii) the adhesive was assumed to fail wherever the peel stress was tensile—this represented a condition by which at least 50% of the glue line had failed.

The results of these analyses can be found in Table 4 as can the result for the case when the hole was unfilled. This shows that in each case the adhesively-bonded rivet has dramatically reduced the stresses around the hole and thus a significant increase in the life to crack initiation could be expected.

Attention is now directed to the situation when the hole is cracked. Cracks of various discrete depths, up to a maximum of 2·5 mm, were considered for the following cases:

(i) a through crack on one side of the hole only (half the structure modelled),

(ii) through cracks of equal depth, on each side of the hole (a quarter of the structure modelled).

The finite element model for these problems consisted of approximately 74 eight-noded isoparametric quadrilateral elements and 32 six-noded isoparametric triangular elements for case (i) and 36 and 24 respectively for case (ii) (see Fig. 10(*b*)). As before, reduced integration was used and the solution was performed in double precision. The results of this analysis are given in Tables 5 and 6. Also given are the values of the stress intensity factor for the case when the hole is unfilled and for the case when there is a crack but no rivet hole. The results for the double-sided crack case are shown plotted in Fig. 11.

There are a number of important points indicated by this analysis:

(i) A bonded rivet significantly reduces the stress intensity factor, even after a significant proportion of the adhesive has failed. Thus the use of adhesive-bonded rivets would be expected to result in reduced fatigue-crack propagation rates.

(ii) The values of stress intensity factors for the case of a crack on one side and for the case of a crack of the same depth on both sides of the hole are almost identical.

(iii) As the crack depth increases a crack at a bonded rivet hole behaves as if the specimen does not contain a hole. In the present case this asymptotic behaviour is effectively reached at a crack depth of approximately 2·5 mm. This is particularly important since it allows simple, and yet accurate, analytical estimates to be obtained for stress intensity factors of cracked holes which are to be repaired by a bonded insert.

(iv) In the case of a crack on both sides of the hole the value of the stress intensity factor for a 3·0 mm crack at a bonded rivet hole (with adhesive failed in tension) is approximately the same as for a 0·5 mm crack at an unfilled rivet hole.

Whilst this summary of the finite element analysis has concentrated on bonded rivets with a particular adhesive thickness, the more detailed investigation presented in Ref. 10 covers the effects of variable adhesive thickness and the use of a bonded sleeve in larger fastener bolts.

A comparison of the results of the finite element analyses for cracked specimens and the data obtained from the fractographic analysis indicates that the finite element analysis successfully predicts the observed trends. Referring to the data in Table 3 and Fig. 11 for the open hole and adhesively-bonded rivet (adhesive failed) specimens, a 50% reduction in observed fatigue crack propagation rates between pairs of crack depths corresponds to about 17% reduction in the stress intensity factors for both types of specimens. This value of 17% is in excellent agreement with that obtained from Ref. 9. However, the effective reduction in stress intensity at any given crack depth as a result of the insertion of an adhesively-bonded rivet is much less than that predicted by the finite element analysis. For example, at a crack depth of 0·5 mm the 50% reduction in crack propagation rate would suggest a reduction in stress intensity of about 17%, whereas the finite element analysis predicts a reduction of greater than 50%.

Clearly the finite element model for determining stress intensities incorporated a number of simplifying assumptions of which the geometry of the crack front relative to those which developed in actual fatigue specimens and the characteristics of the glue line are probably the most significant. If one assumes that there are fewer uncertainties in representing the situation for an unfilled hole, then (on a relative basis) the major reason for the discrepancies between actual and predicted stress intensities for the open-hole specimens and those incorporating adhesively-bonded rivets is in the adequacy of the model for defining the properties and behaviour of the adhesive. Nevertheless, the findings outlined in this Report suggest that the concept of adhesively-bonded inserts is worthy of a more detailed study.

5. CONCLUSIONS

1. The insertion of close-fit adhesively-bonded rivets in holes can provide significant improvements in fatigue life compared with that for specimens having open holes.

2. For small crack depths the rates of fatigue crack propagation in adhesively-bonded rivet specimens are only about half those in open-hole specimens.

3. Finite element analyses indicate that adhesive bonding significantly reduces both the local stress concentration at the hole and the stress intensities at the crack tips, thus retarding crack initiation and reducing fatigue crack propagation rates.

4. The effective reduction in stress intensity resulting from bonding (about 17%) is much less than the 50% predicted by the finite element analysis. This discrepancy is attributed mainly to shortcomings in the model for defining the characteristics and behaviour of the adhesive.

ACKNOWLEDGEMENTS

The Authors' wish to express their thanks to Dr A. A. Baker of Materials Division for his advice and co-operation, and gratefully acknowledge the assistance of Corporal G. Vejle of the RAAF for bonding the rivets and Messrs W. F. Lupson, G. W. Revill and A. S. Machin of Structures Division for the conduct of the fatigue testing program.

REFERENCES

1. Mann, J. Y., Kalin, R., and Wilson, F. E., Extending the fatigue life of a fighter aircraft wing. *Aircraft fatigue in the Eighties.* (Editors J. B. de Jonge and H. H. van den Linden). Netherlands, National Aerospace Laboratories, 1981, pp. 1.7.1 1.7/42.

2. Mann, J. Y., Machin, A. S., and Lupson, W. F., Improving the fatigue life of the Mirage IIIO wing main spar. *Dept. Defence, Aero. Res. Labs,* Structures Report 398, January 1984.

3. Mann, J. Y., Revill, G. W., and Lupson, W. F., Improving the fatigue performance of thick aluminium alloy bolted joints by cold-expansion and the use of interference-fit steel bushes. *Dept. Defence, Aero. Res. Labs,* Structures Note 486, April 1983.

4. Jones, R., and Callinan, R. J., New thoughts on stopping cracks which emanate from holes. *Int. Jnl Fracture,* Vol. 17, 1981, pp. R53 R55.

5. Gurney, T. R., *Fatigue of welded structures.* Cambridge, Cambridge University Press, 2nd edition, 1979, pp. 334 335.

6. Mann, J. Y., Machin, A. S., Lupson, W. F., and Pell, R. A., The use of interference-fit bolts or bushes and hole cold-expansion for increasing the fatigue life of thick-section aluminium alloy bolted joints. *Dept. Defence, Aero. Res. Labs,* Structures Note 490, August 1983.

7. Phillips, J. L., Fatigue improvement by sleeve cold-working. *SAE Paper* No. 73095, October 1973.

8. Mann, J. Y., and Jost, G. S., Stress fields associated with interference-fitted and cold-expanded holes with particular reference to the fatigue life enhancement of aircraft structural joints. *Metals Forum,* Vol. 6, No. 1, 1983, pp. 43 53.

9. Finney, J. M. *et al.,* Modelling for fatigue crack growth prediction in Mirage IIIO frame 26. *Dept. Defence, Aero. Res. Labs,* Structures Report 401, April 1984.

10. Jones, R., and Heller, M., On the stress analysis of bonded inserts. *Dept. Defence, Aero. Res. Labs,* Structures Report 000, 1984.

APPENDIX 1

Properties of Test Materials

(a) Chemical composition (%)

Element	British Standard L168 : 1978	Test Material GR	QQ-A-255a (2014)	Test Material GJ
Cu	3.9–5.0	4.29	3.9–5.0	4.48
Mg	0.2–0.8	0.43	0.2–0.8	0.60
Mn	0.4–1.2	0.76	0.4–1.2	0.91
Fe	0.5 max.	0.23	1.0 max.	0.45
Si	0.5–0.9	0.74	0.5–1.2	0.86
Ti	0.15 max.	not analyzed		not analyzed
Cr	0.10 max.	0.01	0.1 max.	0.04
Zn	0.25 max.	<0.20	0.25 max.	0.12

(b) Static tensile properties

Property	British Standard L168 : 1978	Test material GR	QQ-A-255a (2014-T651) (transverse)	Test material GJ (transverse)	Test material GJ (longitudinal)
0.1% proof stress (MPa)		466		458	470
0.2% proof stress (MPa)	440	474	407 (59 000 psi)	466	475
Ultimate tensile stress (MPa)	490	524	462 (67 000 psi)	506	509
Elongation (%)	7	11	4	8.5	9.3
0.1% proof / ultimate		0.89		0.91	0.92

(c) Fracture toughness (K_{Ic})

	Test material GR*	Test material GJ†
MPa m$^{1/2}$	32.0	25.0
ksi in$^{1/2}$	29.2	22.8

* Average of five tests on 19 mm thick compact tension specimens.
† Average of five tests on 25 mm thick compact tension specimens.

APPENDIX 2

Hole Treatments

The holes in all specimens were initially drilled at 3·3 mm diameter (from the Datum Face), and countersunk 120°, 5·5 mm diameter at the Datum Face. Final reaming for all except Type (a) and (a) specimens was 4·010/4·028 mm diameter, also from the Datum Face.

A Boeing split sleeve cold-expansion

Starting hole size	3·683/3·708 mm
Finished hole size (after reaming)	4·010/4·028 mm
Degree of cold-expansion	2·7 to 3·4%
Direction of expansion	Toward Datum Face

(Elastic recovery of the test specimen material occurs after withdrawal from the hole of the cold-expansion tool. The degree of cold-expansion is defined as the percentage difference in diameter between the starting hole size, and the maximum mandrel diameter plus twice the sleeve thickness.)

B Adhesive bonding

The surface treatment of the holes consisted of a thorough degreasing using Methyl Ethyl Ketone followed by light abrasion using a stainless steel wire brush. Adhesive type K138 (a two-part epoxy manufactured by CIBA) was then applied to the surfaces of the hole and the rivet, and the rivet worked into the hole to ensure that the surfaces of both the hole and the rivet were fully coated. The adhesive was then cured overnight at 40°C.

APPENDIX 3

Fractographic Crack Growth Measurements

Each fracture was examined using three independent techniques:

(i) a macrophotograph at about ×15 magnification to provide crack growth data at relatively large crack depths,

(ii) an optical stereo microscope with diffuse illumination and magnifications of ×100, 50 and 25, and

(iii) a metallographic microscope with polarized vertical illumination, using magnifications of ×500 or 50.

Both microscopes were fitted with a cross-hair in one eye piece. The specimens were mounted on an X-Y stage fitted with photo-electrical digital micrometers reading to 0.001 mm, and the crack depths corresponding to the applications of the 7.5 g load were accurately measured by traversing the specimens under the microscope objectives. Whenever possible the traverse of the fracture surface was perpendicular to the axis of the hole.

Because of the substantial overlapping of the region of the fracture by each independent visualization technique about 80% of the crack depth data were duplicated. However, measurements obtained using the metallographic microscope were considered to be the most accurate at short crack depths (×500) and large crack depths (×50), and those using the stereo microscope the most accurate at intermediate crack depths. Thus the crack depth versus life data presented are not a simple average of the measurements obtained by the different techniques but represent the actual measurements obtained using the technique considered to be most accurate over particular regions of the fracture. When combined together they provided a coherent set of data covering the entire line of traverse.

As a check on the validity of the interpretation of the individual fracture markings on each specimen all the data obtained for a particular fracture using the three independent techniques were combined and examined on the basis of a relationship between crack depth and incremental crack growth. For intermediate and large crack depths (e.g. for greater than about 0.5 mm) this relationship was found to be approximately linear. On the relatively rare occasions when individual measurements indicated wide departures from this relationship the particular data were reassessed. When data could not be validated by independent measurements using more than one technique (about 20% of the data), the validity of individual measurements in such cases were assessed by the individual relationship between crack depth and incremental crack growth.

TABLE 1

Fatigue test results, Type (a) specimens

Hole treatment	Specimen No. GR	Life (flights)
(i) Drilled 3·3 mm, filled 1/8 inch rivets	18F	9,542
	13B	10,042
	19C	10,320
	log. average life	9,963
	s.d. log. life	0·017
(ii) Drilled 3·3 mm, open holes	26B	7,500
	16F	8,105
	log. average life	7,797
	s.d. log. life	0·024
(iii) Reamed 4 mm, open holes	25B	5,542
	18B	6,342
	log. average life	5,929
	s.d. log. life	0·041
(iv) Reamed 4 mm, pressed-in 5/32 inch rivets	17B	3,735
	23B	3,842
	14B	6,335
	log. average life	4,496
	s.d. log. life	0·129
(v) Reamed 4 mm, adhesive-bonded 5/32 inch rivets	20B	14,642
	13C	16,040
	16B	16,440
	log. average life	15,688
	s.d. log. life	0·026
(vi) Expanded 4 mm, open holes	19B	7,142
	24B	9,442
	log. average life	8,212
	s.d. log. life	0·086
(vii) Expanded 4 mm, pressed-in 5/32 inch rivets	17C	5,942
	14F	7,642
	21B	8,080
	log. average life	7,159
	s.d. log. life	0·071
(viii) Expanded 4 mm, adhesive bonded 5/32 inch rivets	15B	10,542
	22B	23,542
	15C	26,130
	log. average life	18,648
	s.d. log. life	0·216

TABLE 2

Fatigue test results, Type (b) specimens

Hole treatment	Specimen No. GJ	Life (flights)
(i) Reamed 4 mm. open holes	1U	2,542
	1ZB	3,242
	log. average life	2,871
	s.d. log. life	0·075
(ii) Reamed 4 mm. open holes coated with adhesive	1Y	2,742
	1V	2,842
	log. average life	2,792
	s.d. log. life	0·011
(iii) Reamed 4 mm. pressed-in rivet	2A16	3,542
	1Z	3,820
	log. average life	3,678
	s.d. log. life	0·023
(iv) Reamed 4 mm. adhesive-bonded rivet	1X	5,742
	1ZA	7,942
	2B16	8,942
	log. average life	7,415
	s.d. log. life	0·100

TABLE 3

Crack Propagation Rates Determined from Fractographic Measurements

Crack depth (mm)	Crack propagation rate (mm/100 flights)		Reduction in rate by bonding (%) $[(1 - B/A) \times 100]$
	Open hole specimen GJ1ZB (A)	Bonded rivet specimen GJ2B16 (B)	
0·1	0·026	0·0001	99·6
0·2	0·038	0·009	76
0·3	0·052	0·019	63
0·4	0·065	0·028	57
0·5	0·080	0·039	51
0·6	0·094	0·049	48
0·7	0·109	0·060	45
0·8	0·125	0·071	43
0·9	0·141	0·082	42
1·0	0·158	0·094	41
1·1	0·175	0·106	39
1·2	0·193	0·119	38
1·3	0·211	0·131	38
1·4	0·229	0·144	37
1·5	0·248	0·158	36
1·6	0·268	0·172	36
1·7	0·288	0·186	35
1·8	0·308	0·200	35
1·9	0·329	0·215	35
2·0	0·351	0·230	35
2·1	0·373	0·245	34
2·2	0·395	0·261	34
2·3	0·418	0·277	34
2·4	0·441	0·293	34
2·5	0·465	0·310	33

TABLE 4

Maximum principal stress for the uncracked specimen

Case considered	Stress (MPa)
Unfilled hole	853
Bonded rivet (no adhesive failure)	337
Bonded rivet (adhesive failed in tension)	427

TABLE 5

Stress Intensity Factors K (MPa $m^{1/2}$) for a cracked hole—crack on one side only

Crack depth (mm)	Bonded rivet		No hole	Open hole
	No adhesive failure	Adhesive failed in tension		
0·5	9·1	12·1		25·6
0·9	11·3	15·0		27·8
1·5	14·3	18·4	13·1	29·9
2·0	15·9	20·1	14·8	30·9
2·3	17·1	21·4	16·0	32·1

TABLE 6

Stress Intensity Factors K (MPa $m^{1/2}$) for a cracked hole—for a crack on both sides

Crack depth (mm)	Bonded rivet		Open hole
	No adhesive failure	Adhesive failed in tension	
0·5	9·1	12·2	26·4
0·9	11·3	15·3	29·7
1·5	14·5	18·8	33·9
2·3	17·6	22·6	39·2
2·5		23·6	

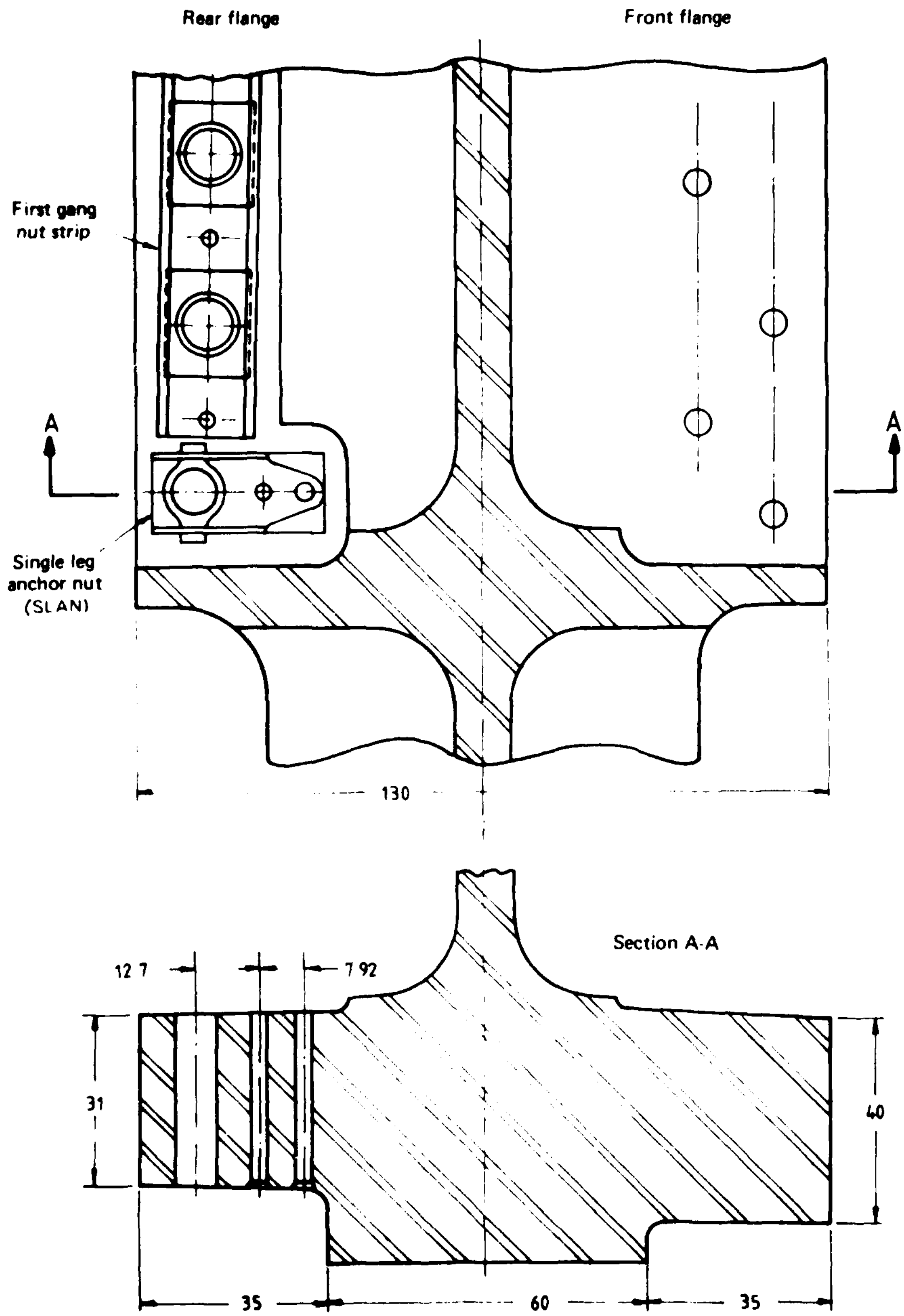

FIG. 1 MIRAGE $\overline{111}$0 SPAR – LOWER SURFACE AT SLAN SECTION

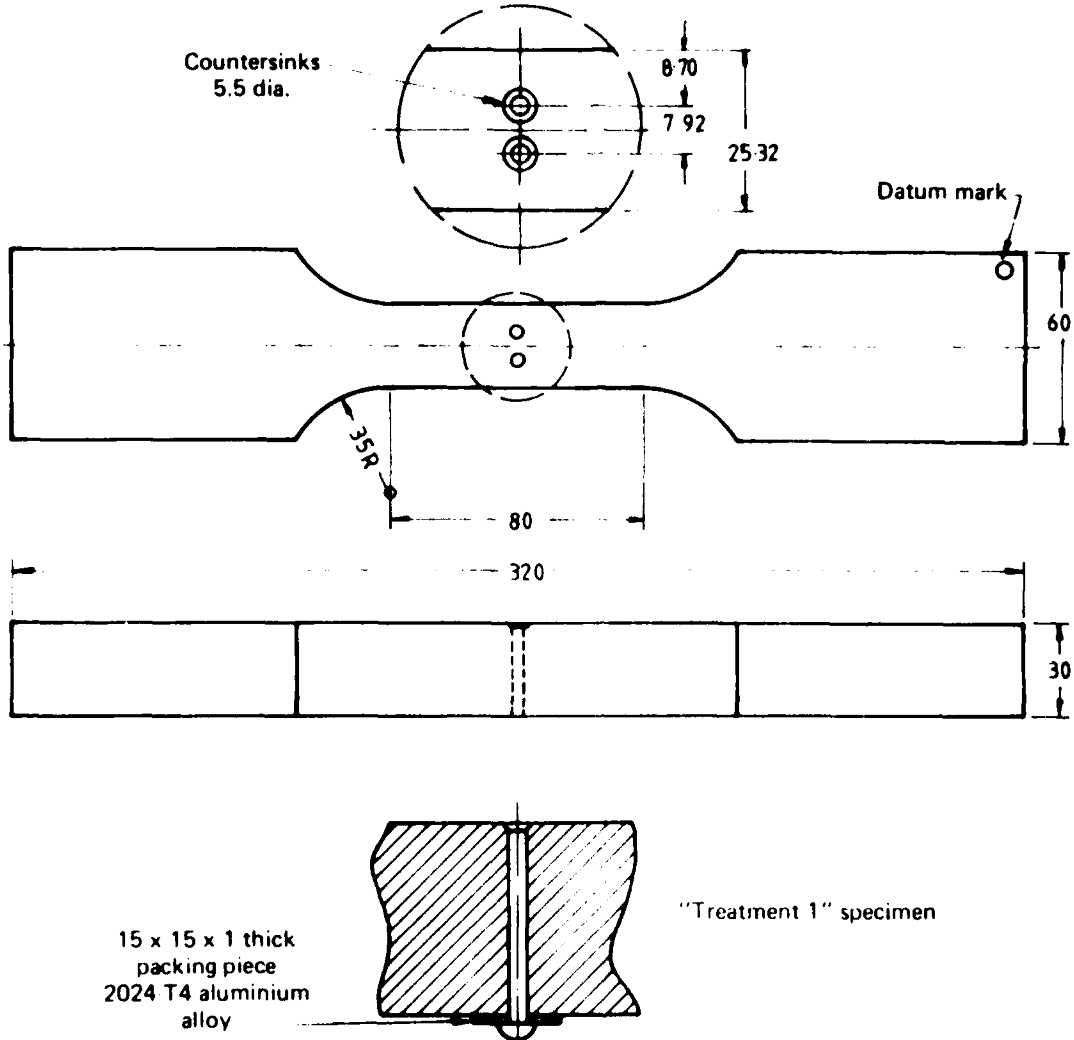

(a) Twin SLAN rivet hole specimen

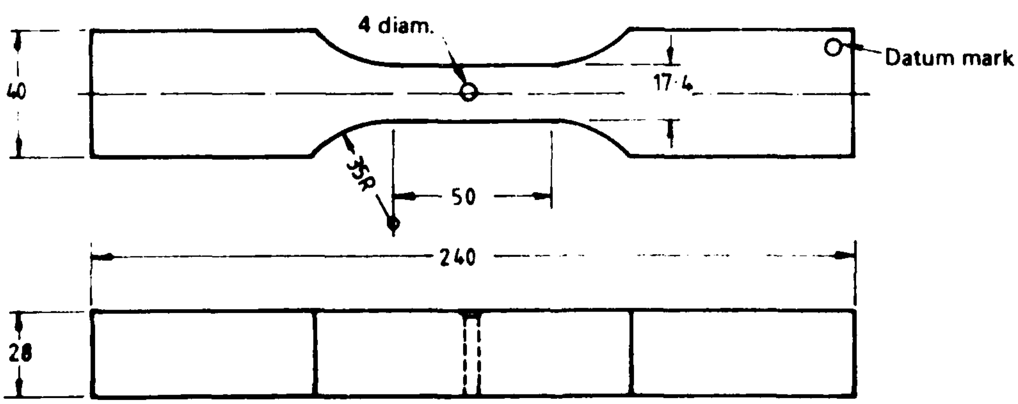

(b) Single SLAN rivet hole specimen

FIG. 2 FATIGUE TEST SPECIMENS
(all dimensions in mm)

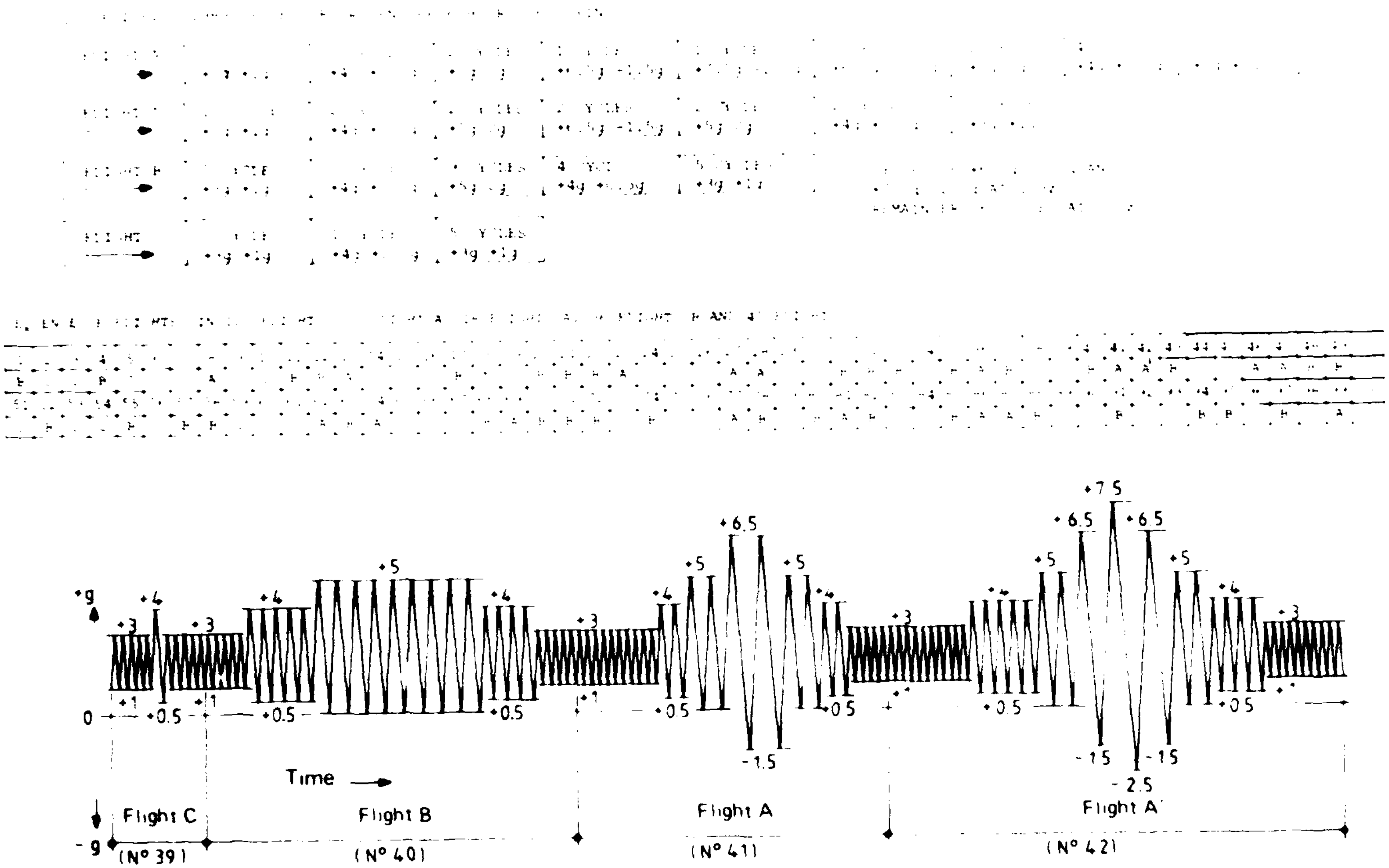

FIG. 3 FRENCH 100 FLIGHT MIRAGE III FLIGHT-BY-FLIGHT SEQUENCE

Specimen No. GR18E
Flights 9,542

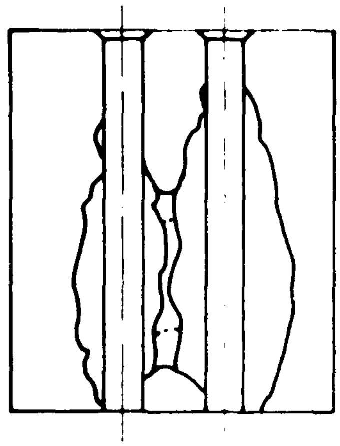

Specimen No. GR13B
Flights 10,042

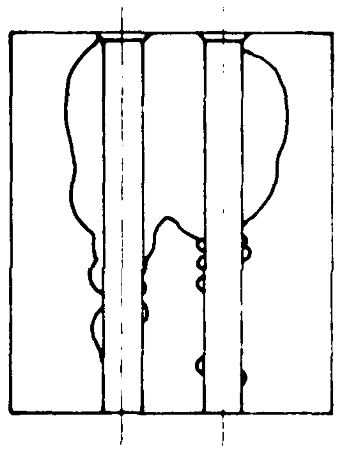

Specimen No. GR19C
Flights 10,320

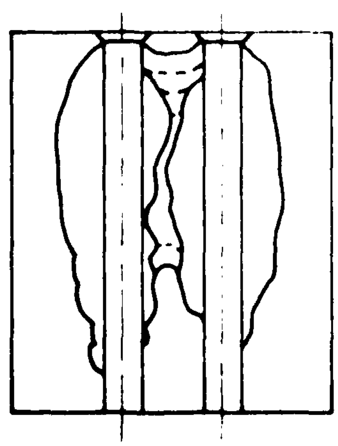

FIG 4 (i) FRACTURES TYPE (ai) SPECIMENS. DRILLED 3.3 mm, FILLED 0.125 in. RIVETS

Specimen No. GR26B
Flights 7,500

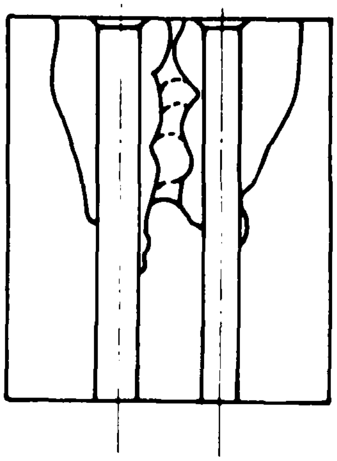

Specimen No. GR16E
Flights 8,105

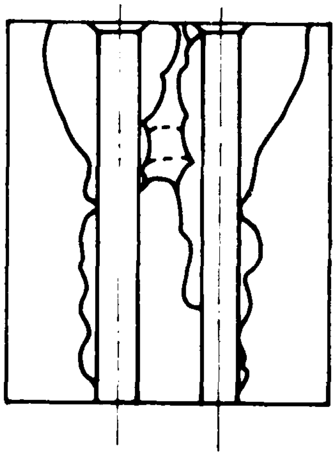

FIG. 4 (ii) FRACTURES TYPE (aii) SPECIMENS. DRILLED 3.3 mm, OPEN HOLES

Specimen No. GR25B
Flights 5,542

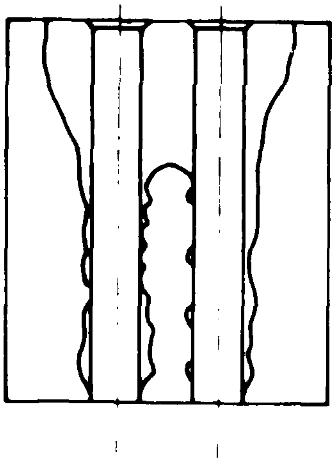

Specimen No. GR18B
Flights 6,342

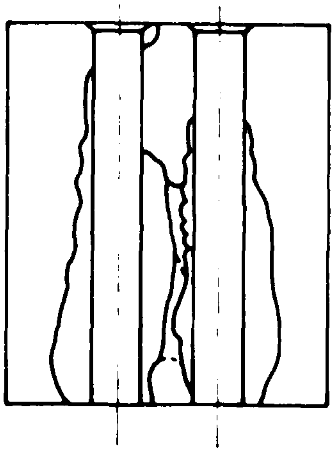

FIG. 4 (iii) FRACTURES TYPE (aiii) SPECIMENS. REAMED 4 mm, OPEN HOLES

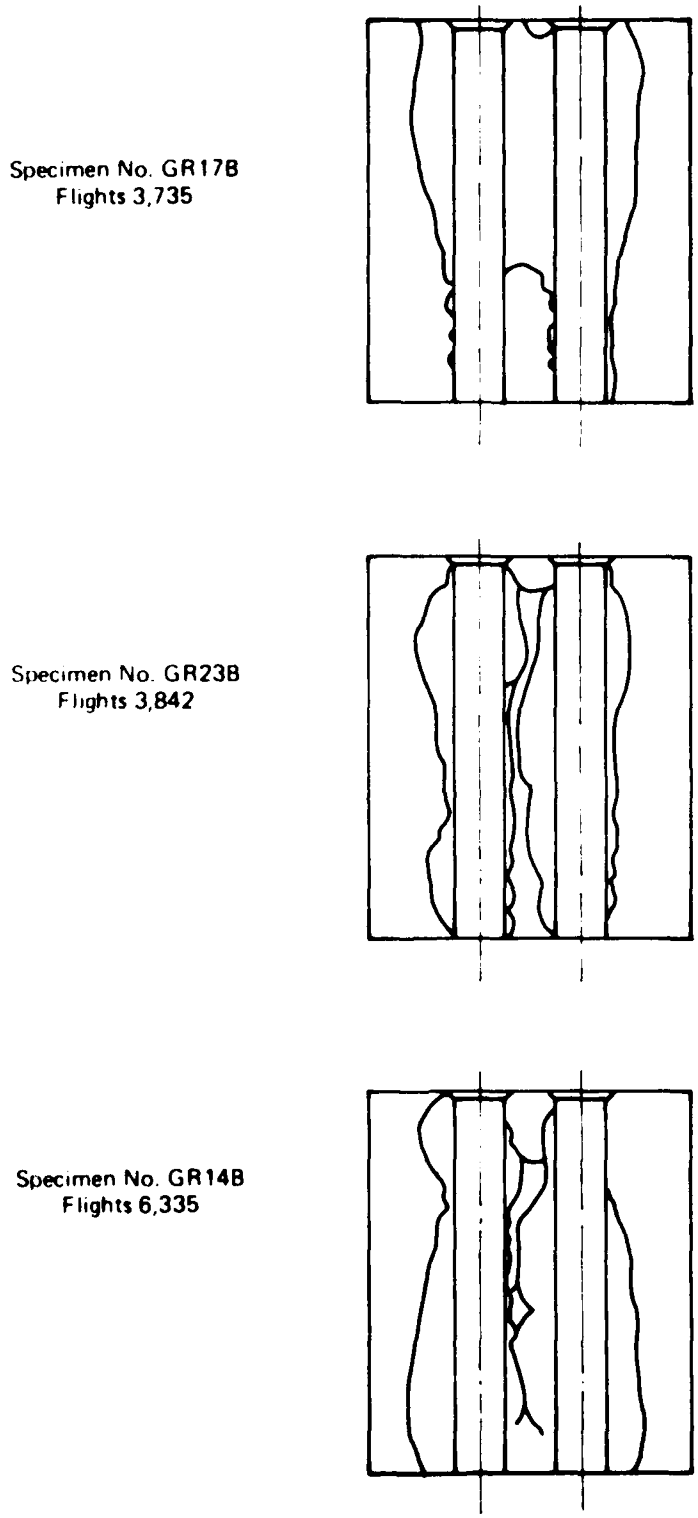

FIG. 4 (iv) FRACTURES TYPE (aiv) SPECIMENS. REAMED 4 mm, PRESSED-IN $^{5}/_{32}$ in. RIVETS

Specimen No. GR20B
Flights 14,642

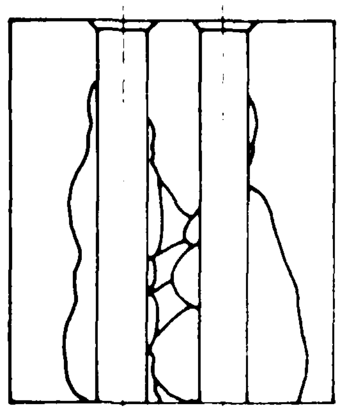

Specimen No. GR13C
Flights 16,040

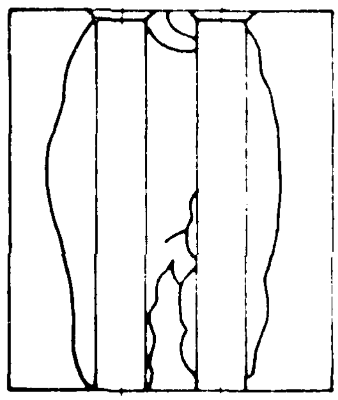

Specimen No. GR16B
Flights 16,440

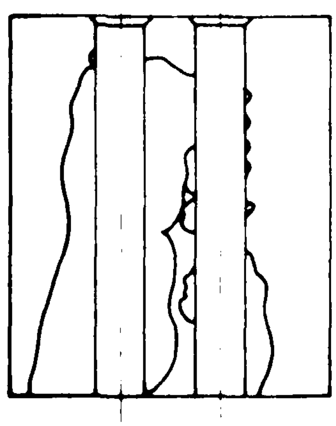

FIG 4 (v) FRACTURES TYPE (av) SPECIMENS. REAMED 4 mm, ADHESIVE BONDED $^{5}/_{32}$ in. RIVETS

Specimen No. GR19B
Flights 7,142

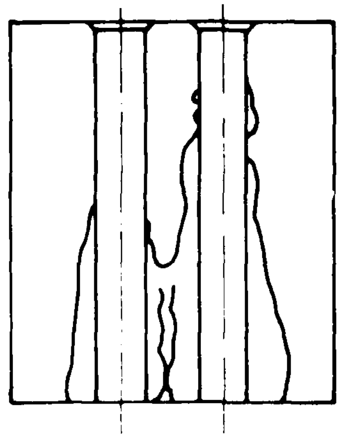

Specimen No. GR24B
Flights 9,442

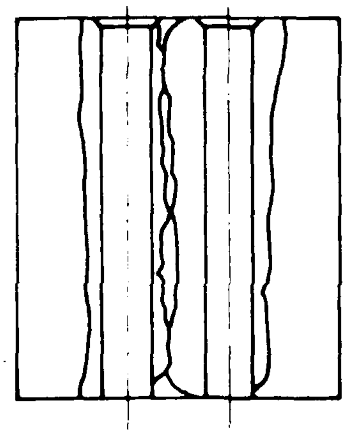

FIG. 4 (vi) FRACTURES TYPE (avi) SPECIMENS. COLD-EXPANDED 4 mm, OPEN HOLES

Specimen No. GR17C
Flights 5,942

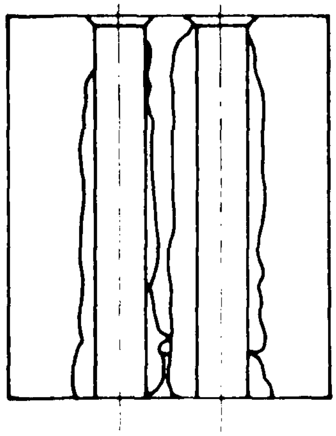

Specimen No. GR14E
Flights 7,642

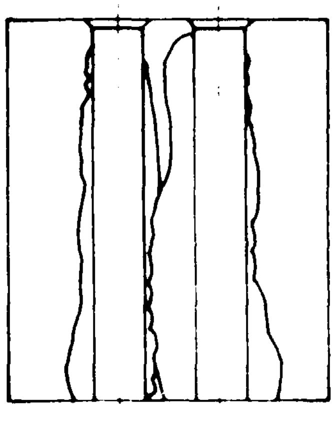

Specimen No. GR21B
Flights 8,080

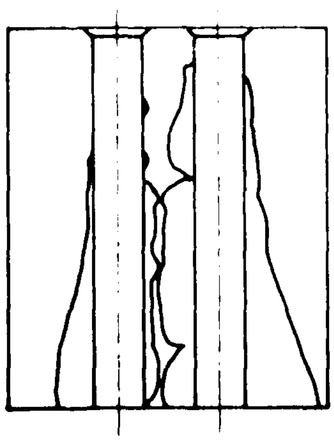

FIG. 4 (vii) FRACTURES TYPE (avii) SPECIMENS. COLD EXPANDED 4 mm, PRESSED-IN $^5/_{32}$ in. RIVETS

Specimen No. GR15B
Flights 10,542

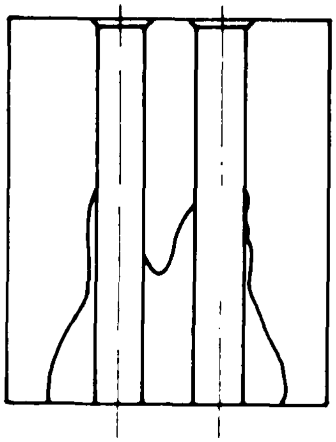

Specimen No. GR22B
Flights 23,542

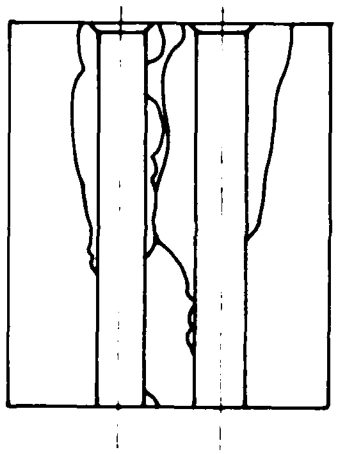

Specimen No. GR15C
Flights 26,130

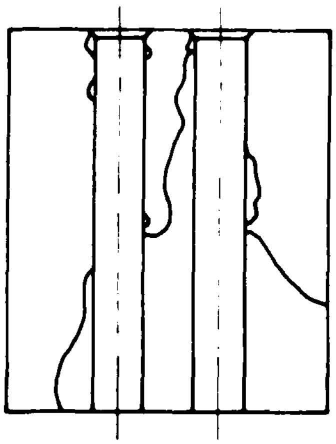

FIG. 4 (viii) FRACTURES TYPE (aviii) SPECIMENS. COLD EXPANDED 4 mm, ADHESIVE BONDED $^{5}/_{32}$ in. RIVETS

Specimen No. GR18E
Type (ai) – 3.3 mm
drilled holes, 0.125
in. rivets

Specimen No. GR16E
Type (aii) – 3.3 mm
drilled holes, open

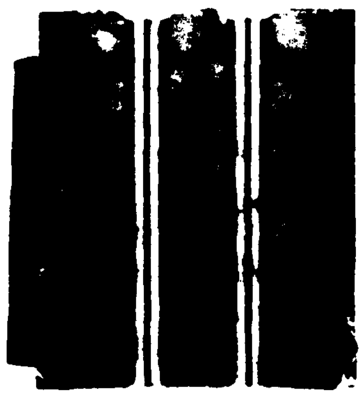

Specimen No. GR18B
Type (aiii) – 4 mm
reamed holes, open

FIG. 5 (a) FRACTURE SURFACES TYPE (a) SPECIMENS

Specimen No. GR14B
Type (aiv) – 4 mm
reamed holes, pressed
in rivets

Specimen No. GR13C
Type (av) - 4 mm
reamed holes, adhesive
bonded rivets

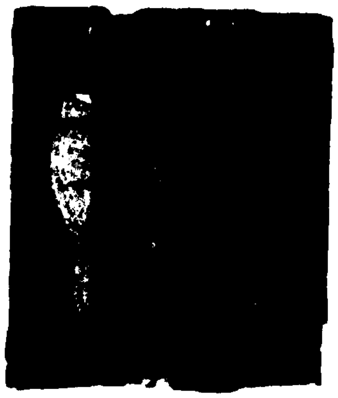

Specimen No. GR24B
Type (avi) – 4 mm
cold expanded holes,
open

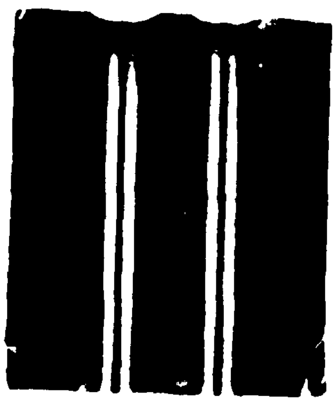

FIG. 5 (b) FRACTURE SURFACES TYPE (a) SPECIMENS

Specimen No. GR14E
Type (avii) – 4 mm
cold expanded holes,
pressed-in rivets

Specimen No. GR22B
Type (aviii) – 4 mm
cold-expanded holes,
adhesive-bonded
rivets

FIG. 5 (c) FRACTURE SURFACES TYPE (a) SPECIMENS

Specimen No. GJ1U
Flights 2,542

(i)

Specimen No. GJ1ZB
Flights 3,242

Specimen No. GJ1Y
Flights 2,742

(ii)

Specimen No. GJ1V
Flights 2,842

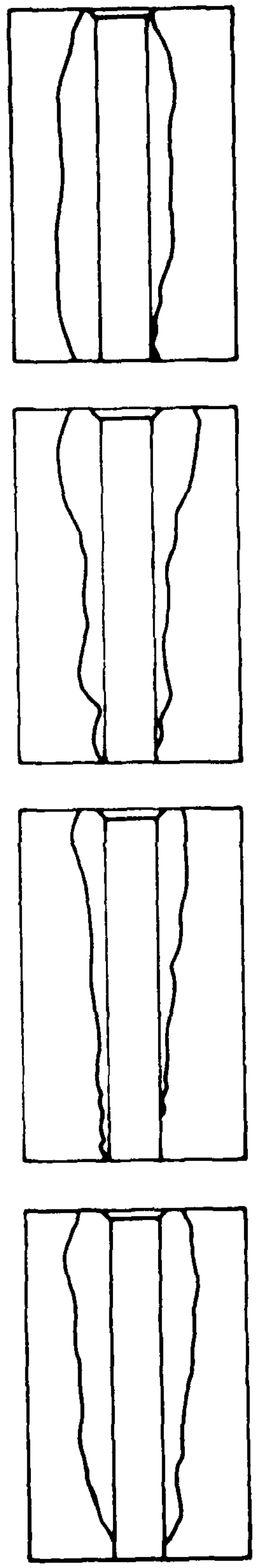

FIG. 6 FRACTURES TYPE (b) SPECIMENS.
(i) Reamed 4 mm, open holes, and
(ii) Reamed 4 mm, open holes adhesive coated

Specimen No. GJ2A16
Flights 3,542

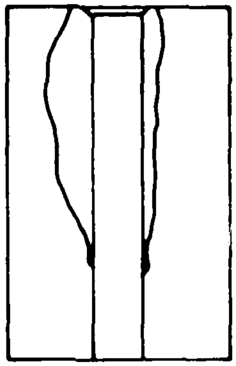

Specimen No. GJ1Z
Flights 3,820

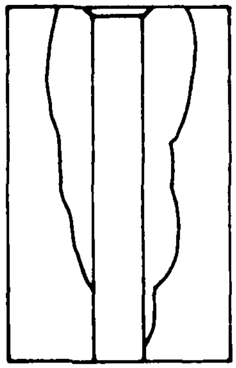

FIG. 6 (iii) FRACTURES TYPE (biii) SPECIMENS.
Reamed 4 mm, pressed-in rivet

Specimen No. GJ1X
Flights 5,742

Specimen No. GJ1ZA
Flights 7,942

Specimen No. GJ2B16
Flights 8,942

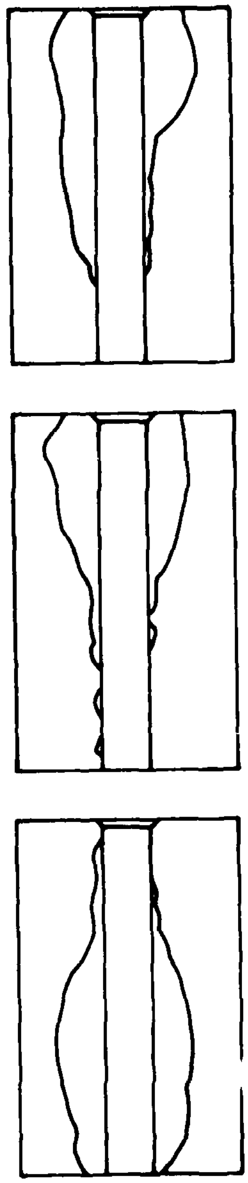

FIG. 6 (iv) FRACTURES TYPE (biv) SPECIMENS.
Reamed 4 mm, adhesive-bonded rivet

Specimen No. GJ1ZB
Type (bi) – 4 mm
reamed hole, open

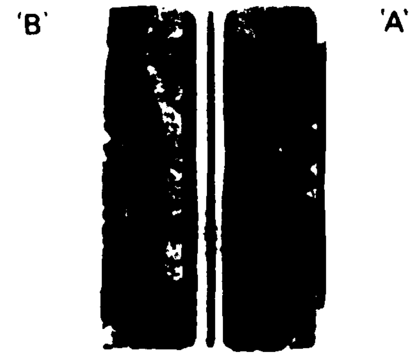

Specimen No. GJ1Y
Type (bii) – 4 mm
reamed hole, adhesive
coated, open

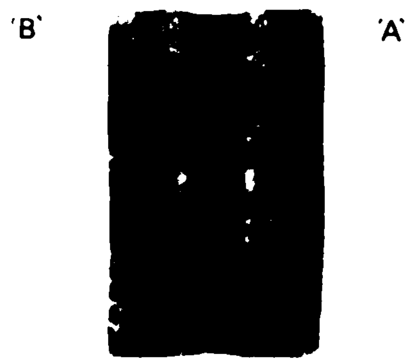

Specimen No. GJ2A16
Type (biii) – 4 mm
reamed hole, pressed-in
rivet

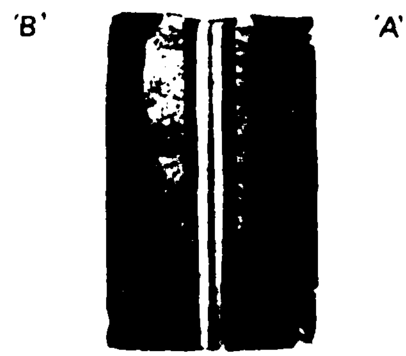

Specimen No. GJ2B16
Type (biv) – 4 mm
reamed hole, adhesive
bonded rivet

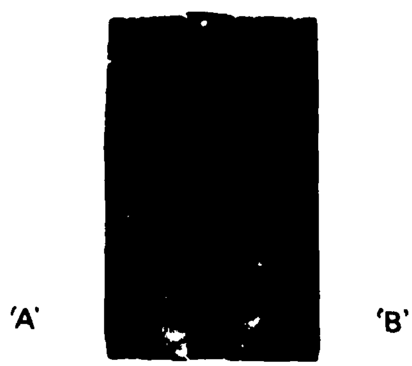

FIG. 7 FRACTURE SURFACES TYPE (b) SPECIMENS

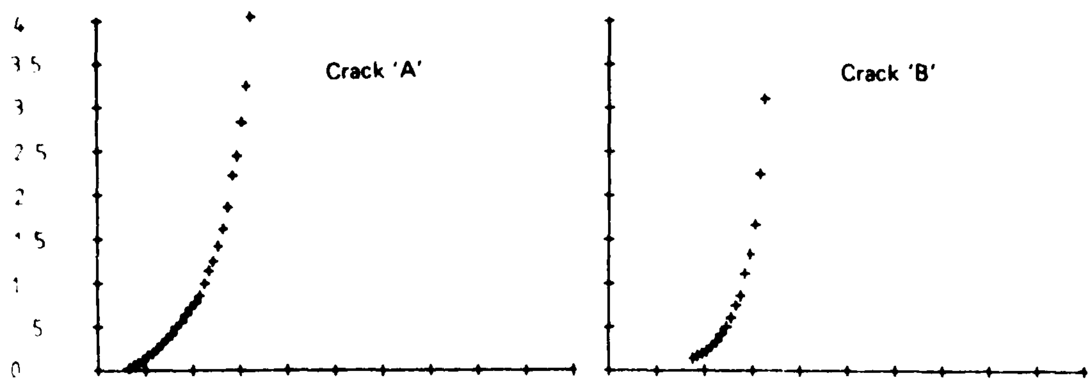

(a) Specimen GJ1ZB – 4 mm reamed hole, open

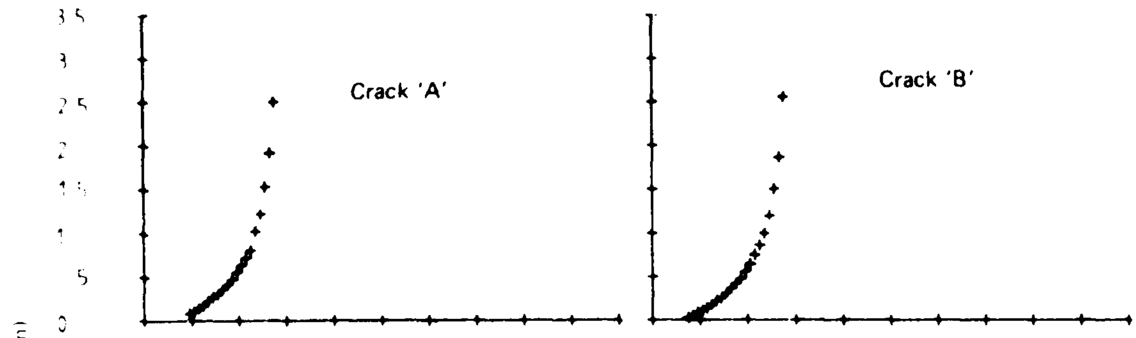

(b) Specimen GJ1Y – 4 mm reamed hole, adhesive coated, open

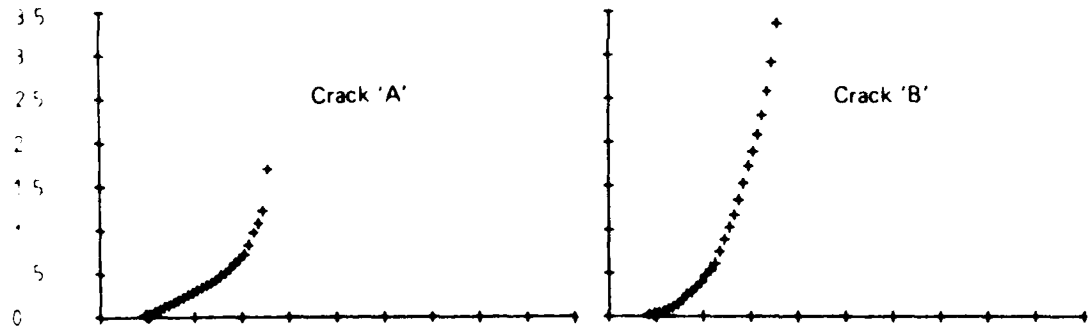

(c) Specimen GJ2A16 – 4 mm reamed hole, pressed in rivet

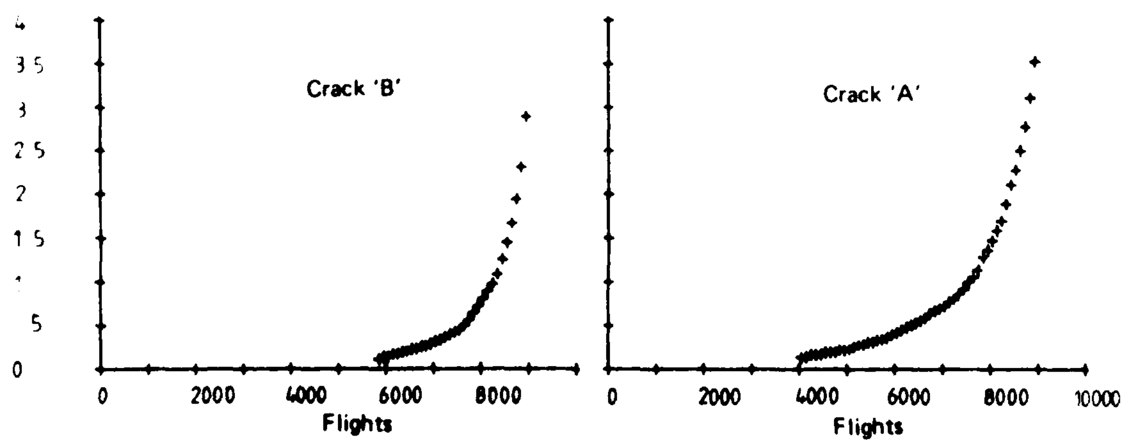

(d) Specimen GJ2B16 – 4 mm reamed hole, adhesive-bonded rivet

FIG. 8 (ii) CRACK PROPAGATION, TYPE (b) SPECIMENS

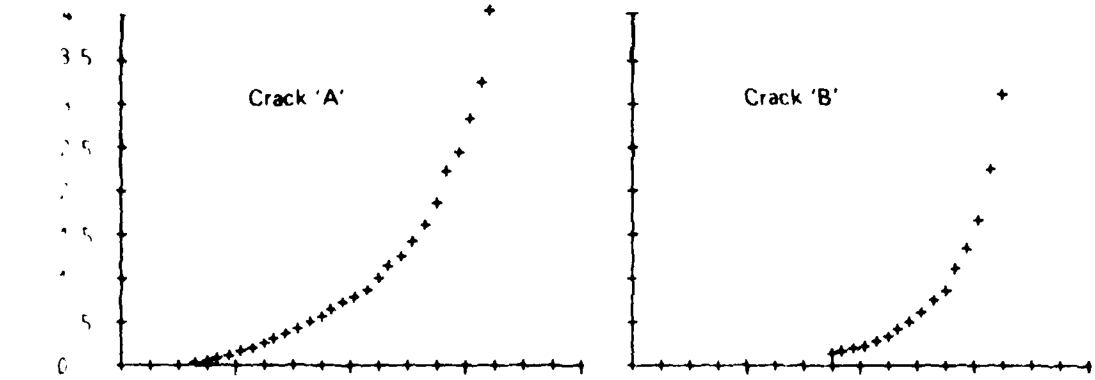

(a) Specimen GJ1ZB – 4 mm reamed hole, open

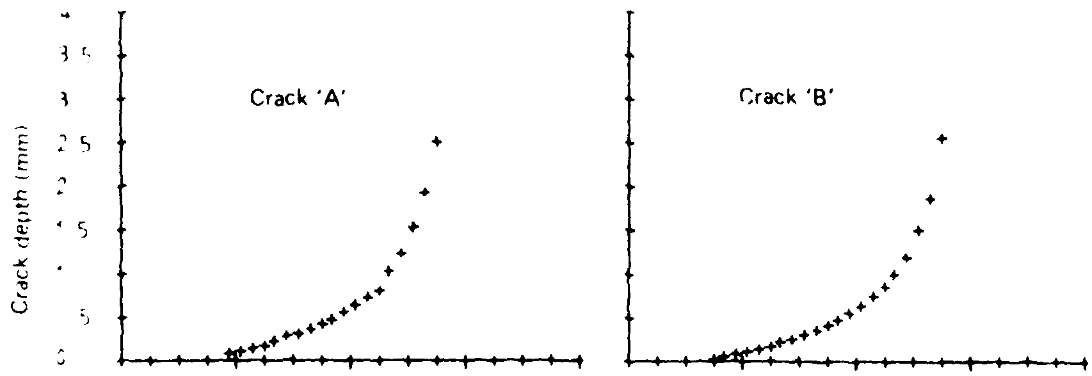

(b) Specimen GJ1Y 4 mm reamed hole, adhesive coated, open

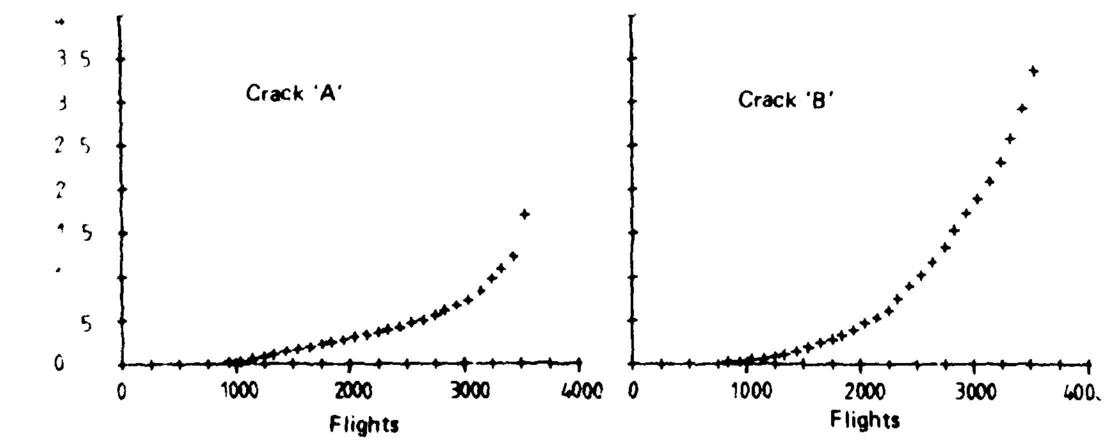

(c) Specimen GJ2A16 – 4 mm reamed hole, pressed-in rivet

FIG. 8 (i) CRACK PROPAGATION, TYPE (b) SPECIMENS

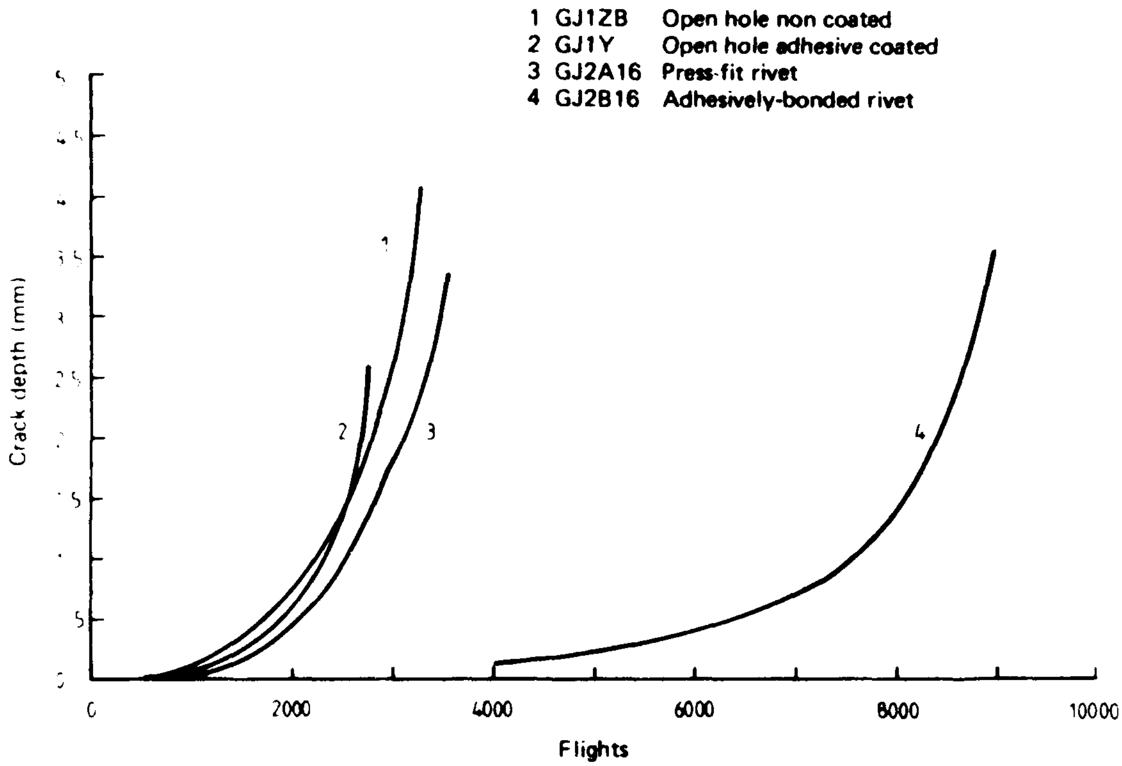

FIG. 9 CRACK PROPAGATION, TYPE (b) SPECIMENS

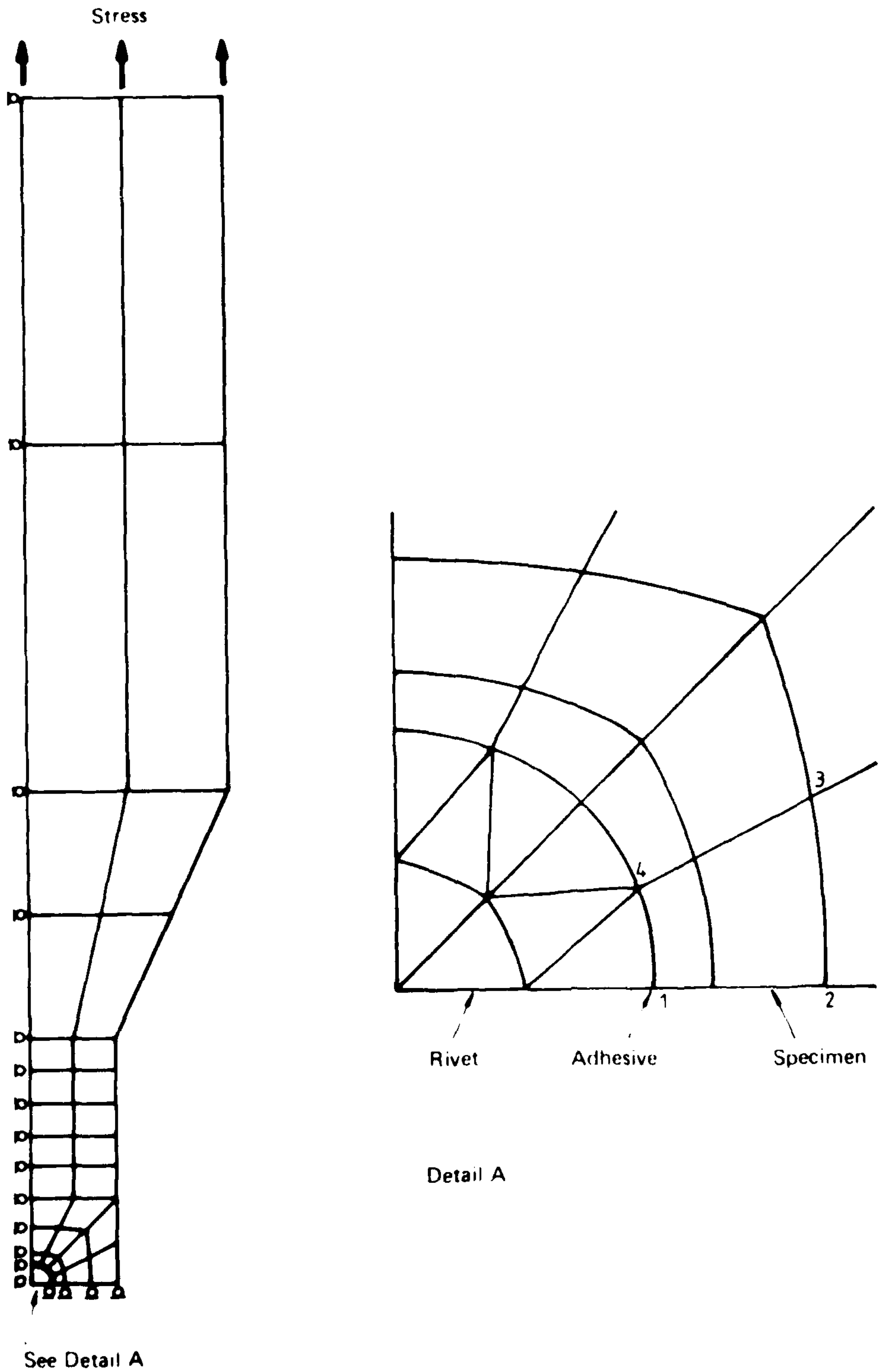

FIG. 10 (a) FINITE ELEMENT MESH FOR UNCRACKED SPECIMEN – BONDED RIVET

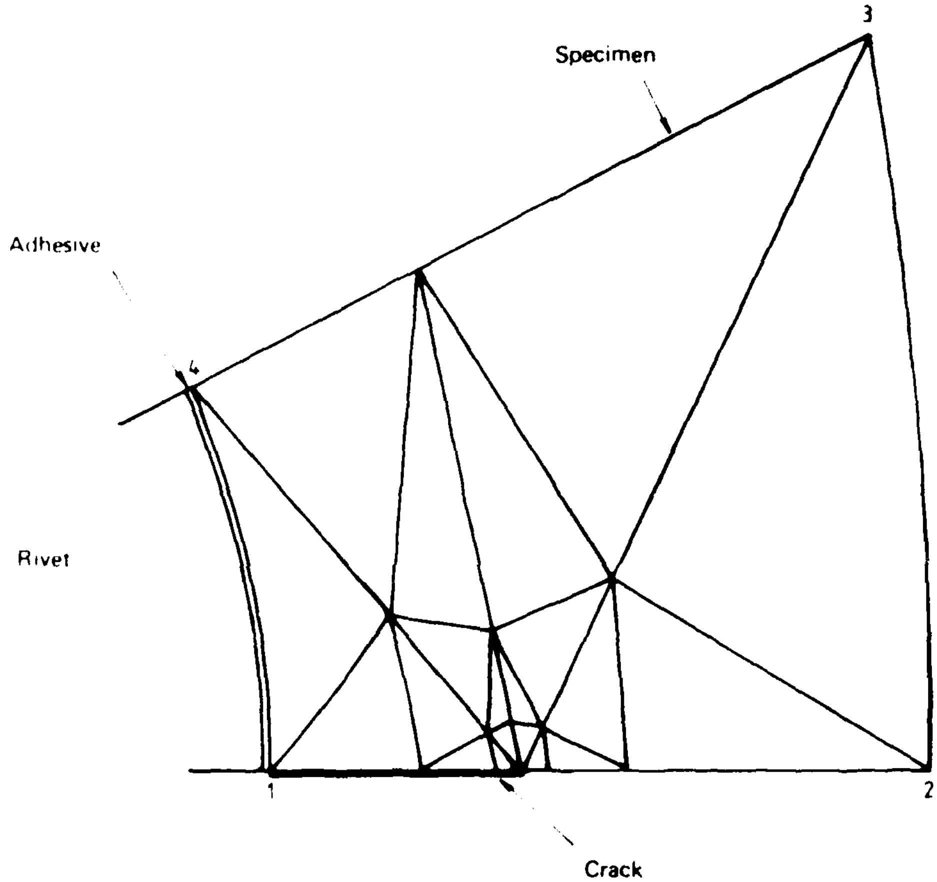

FIG. 10 (b) FINITE ELEMENT MESH FOR CRACKED SPECIMEN – BONDED RIVET
(ONLY MESH IN REGION OF CRACK FOR QUARTER SECTION SHOWN)

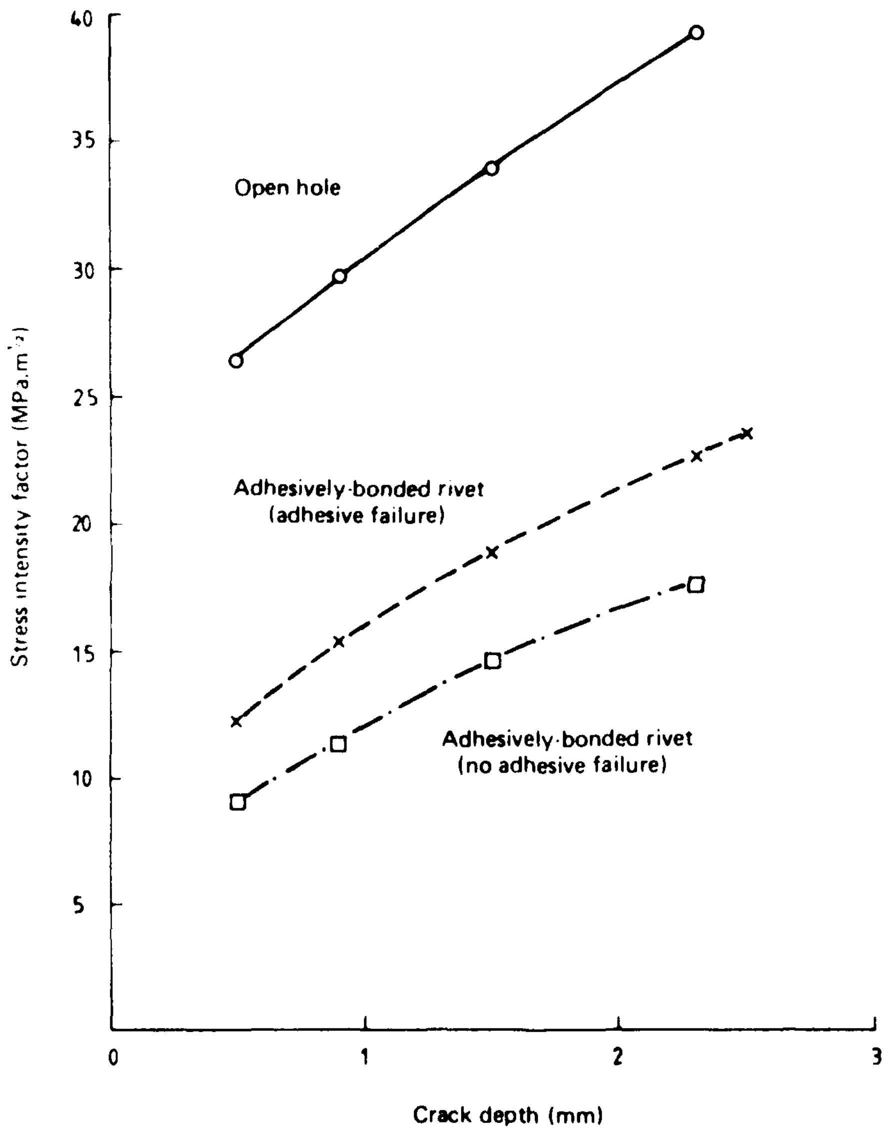

FIG. 11 STRESS INTENSITY FACTORS FOR HOLES WITH CRACKS ON BOTH SIDES

DISTRIBUTION

AUSTRALIA

DEPARTMENT OF DEFENCE

Central Office

Chief Defence Scientist
Deputy Chief Defence Scientist (1 copy)
Superintendent, Science and Technology Programmes
Controller, Projects and Analytical Studies
Defence Science Representative (U.K.) (Doc. Data sheet only)
Counsellor, Defence Science (U.S.A.) (Doc. Data sheet only)
Defence Central Library
Document Exchange Centre, D.I.S.B. (18 copies)
Joint Intelligence Organisation
Librarian H Block, Victoria Barracks, Melbourne
Director General - Army Development (NSO) (4 copies)

Aeronautical Research Laboratories

Director
Library
Superintendent - Structures
Superintendent - Materials
Divisional File - Structures
Authors: J. Y. Mann
R. A. Pell
R. Jones
M. Heller
G. S. Jost
A. S. Machin
B.C. Hoskin
J. M. Finney
I. M. Bland
C. K. Rider
J. M. Grandage
J. G. Sparrow
C. A. Patching
A. A. Baker

Materials Research Laboratories

Director/Library

Defence Research Centre

Library

Navy Office

Navy Scientific Adviser
Directorate of Naval Aircraft Engineering

Army Office

Army Scientific Adviser
Engineering Development Establishment, Library

Air Force Office

Air Force Scientific Adviser
Director General Aircraft Engineering - Air Force
HQ Support Command (SLENGO)
Air Attache Paris (Sent direct from ARL)

DEPARTMENT OF DEFENCE SUPPORT

Government Aircraft Factories

Manager
Library

DEPARTMENT OF AVIATION

Library
Flying Operations and Airworthiness Division
Melbourne: Mr K. R. A. O'Brien
Canberra: Mr C. Torkington

STATUTORY & STATE AUTHORITIES AND INDUSTRY

Australian Atomic Energy Commission, Director
CSIRO
Materials Science Division, Library
Trans Australia Airlines, Library
Qantas Airways Limited
SEC of Vic., Herman Research Laboratory, Library
Ansett Airlines of Australia, Library
B.H.P. Melbourne Research Laboratories
Commonwealth Aircraft Corporation
Library
Mr K. J. Kennedy (Manager Aircraft Factory No. 1)
Manager, Design Engineering
Hawker de Havilland Aust. Pty Ltd, Bankstown, Library

UNIVERSITIES AND COLLEGES

Adelaide	Barr Smith Library
Melbourne	Engineering Library
Monash	Hargrave Library
	Professor I. J. Polmear, Materials Engineering
Newcastle	Library
New England	Library
Sydney	Engineering Library
N.S.W.	Metallurgy Library
Queensland	Library
Tasmania	Engineering Library
Western Australia	Library
R.M.I.T.	Library

CANADA

CAARC Coordinator Structures
International Civil Aviation Organization, Library
Energy Mines & Resources Dept
Physics and Metallurgy Research Laboratories
NRC
Aeronautical & Mechanical Engineering Library
Division of Mechanical Engineering, Director

Universities and Colleges

Toronto — Institute for Aerospace Studies

FRANCE

ONERA, Library
AMD-BA
M. Peyrony
D. Chaumette

INDIA

CAARC Coordinator Structures
Defence Ministry, Aero Development Establishment, Library
Hindustan Aeronautics Ltd, Library
National Aeronautical Laboratory, Information Centre

INTERNATIONAL COMMITTEE ON AERONAUTICAL FATIGUE

Per Australian ICAF Representative (25 copies)

ISRAEL

Israel Air Force
Israel Aircraft Industries
Technion-Israel Institute of Technology
Professor J. Singer
Professor A. Buch

JAPAN

National Research Institute for Metals, Fatigue Testing Division
Institute of Space and Astronautical Science, Library

Universities

Kagawa University — *Professor H. Ishikawa*

NETHERLANDS

National Aerospace Laboratory (NLR), Library

Universities

Technological University of Delft — Professor J. Schijve

NEW ZEALAND

Defence Scientific Establishment, Library

RNZAF, Vice Consul (Defence Liason)

Universities

Canterbury	Library
	Professor D. Stevenson, Mechanical Engineering

SWEDEN

Aeronautical Research Institute, Library

Swedish National Defence Research Institute (FOA), Library

SWITZERLAND

Armament Technology and Procurement Group

F + W (Swiss Federal Aircraft Factory)

Mr E. Girard

Dr H. Boesch

Mr A. Jordi

UNITED KINGDOM

Ministry of Defence, Research, Materials and Collaboration

CAARC, Secretary (NPL)

Royal Aircraft Establishment

Bedford, Library

Farnborough, Library

Commonwealth Air Transport Council Secretariat

Admiralty Marine Technology Establishment, Library

National Gas Turbine Establishment

Director, Pyestock North

National Physical Laboratory, Library

National Engineering Laboratory, Library

British Library, Lending Division

CAARC Co-ordinator, Structures

Fulmer Research Institute Ltd, Research Director

Motor Industry Research Association, Director

Rolls-Royce Ltd

Aero Division Bristol, Library

Welding Institute, Library

British Aerospace

Hatfield-Chester Division, Library

British Hovercraft Corporation Ltd, Library

Short Brothers Ltd, Technical Library

Universities and Colleges

Bristol	Engineering Library
Nottingham	Science Library
Southampton	Library
Strathclyde	Library
Cranfield Institute of Technology	Library
Imperial College	Aeronautics Library

UNITED STATES OF AMERICA

NASA Scientific and Technical Information Facility
Applied Mechanics Reviews
Metals Information
The John Crerar Library
The Chemical Abstracts Service
Boeing Co
Mr R. Watson
Mr J. C. McMillan
Lockheed-California Company
Lockheed Georgia
McDonnell Aircraft Company, Library
Nondestructive Testing Information Analysis Center
Fatigue Technology Inc., Mr R. L. Champoux

Universities and Colleges

Iowa	Professor R. I. Stephens
Illinois	Professor D. C. Drucker
Massachusetts Inst of Technology	M.I.T. Libraries
Lehigh University	Professor G. C. Sih, Institute of Solid and Fracture Mechanics

SPARES (15 copies)

TOTAL (195 copies)

Department of Defence

DOCUMENT CONTROL DATA

1. a. AR No. AR 003 011	1. b. Establishment No. ARL STRUC R 399	2. Document Date March 1984	3. Task No. DST 83/005
4. Title THE USE OF ADHESIVE-BONDED RIVETS TO LESSEN THE REDUCTIONS IN FATIGUE LIFE CAUSED BY RIVET HOLES		5. Security a. document Unclassified b. title c. abstract U. U.	6. No. Pages 17 7. No. Refs 10
8. Author(s) J. Y. Mann, R. A. Pell, R. Jones and M. Heller		9. Downgrading Instructions —	
10. Corporate Author and Address Aeronautical Research Laboratories, P.O. Box 4331, Melbourne, Victoria, 3001		11. Authority (as appropriate) a. Sponsor c. Downgrading b. Security d. Approval —	

12. Secondary Distribution (of this document)

Approved for public release

Overseas enquirers outside stated limitations should be referred through ASDIS, Defence Information Services Branch, Department of Defence, Campbell Park, CANBERRA, ACT, 2601

13. a. This document may be ANNOUNCED in catalogues and awareness services available to . . .

No limitations

13. b. Citation for other purposes (i.e. casual announcement) may be (select) unrestricted (or) as for 13 a.

14. Descriptors		15. COSATI Group
Fatigue (materials)	Adhesive bonding	11130
Holes (openings)	Finite element analysis	13050
Stress analysis	Rivets	11010
Cold working	Coatings	

16. Abstract

Rivet holes are potential sites for fatigue crack initiation in aircraft structures. Several methods for improving the life of such details were investigated including coating the surface of the hole with adhesive, cold-expansion of the holes, the insertion of close-fit rivets and the use of adhesively-bonded rivets.

Of the various techniques examined only that involving adhesively-bonded rivets provided any significant improvements in fatigue life. It resulted in a reduction in fatigue crack propagation rate of about 50% compared with that for specimens incorporating open holes.

A finite element analysis indicated that adhesive bonding significantly reduces both the local stress concentration at the hole and the stress intensities at the crack tips, thus retarding crack

This page is to be used to record information which is required by the Establishment for its own use but which will not be added to the DISTIS data base unless specifically requested.

16 Abstract (Contd)

initiation and reducing fatigue crack propagation rates. However, the effective reduction in stress intensity resulting from bonding (about 17%) is much less than the 50% predicted by the finite element analysis. This discrepancy is attributed mainly to shortcomings in the model for defining the characteristics and behaviour of the adhesive.

17 Imprint

Aeronautical Research Laboratories, Melbourne

18 Document Series and Number	19 Cost Code	20 Type of Report and Period Covered
Structures Report 399	257050	—

21 Computer Programs Used

22 Establishment File Ref(s)

—

ATE

LMED

-8